International Journal of Infectious Diseases 56 (2017) 140–154

Contents lists available at ScienceDirect

International Journal of Infectious Diseases

journal homepage: www.elsevier.com/locate/ijid

Review

# Peptide microarray-based characterization of antibody responses to host proteins after bacille Calmette–Guérin vaccination

Davide Valentini[a,b], Martin Rao[b], Lalit Rane[b], Sayma Rahman[c], Rebecca Axelsson-Robertson[a,b], Rainer Heuchel[d], Matthias Löhr[d], Daniel Hoft[e], Susanna Brighenti[c], Alimuddin Zumla[f], Markus Maeurer[a,b,*]

[a] Centre for Allogeneic Stem Cell Transplantation (CAST), Karolinska University Hospital Huddinge, Stockholm, Sweden
[b] Division of Therapeutic Immunology (TIM), Department of Laboratory Medicine (LABMED), Karolinska Institutet, Stockholm, Sweden
[c] Center for Infectious Medicine (CIM), Department of Medicine, Karolinska Institutet, Stockholm, Sweden
[d] Department of Clinical Science, Intervention and Technology (CLINTEC), Karolinska Institutet, Stockholm, Sweden
[e] Division of Immunobiology, Departments of Internal Medicine and Molecular Microbiology, Saint Louis University Medical Centre, Saint Louis, Missouri, USA
[f] Centre for Clinical Microbiology, Division of Infection and Immunity, University College London, and NIHR Biomedical Research Centre, UCL Hospitals NHS Foundation Trust, London, UK

ARTICLE INFO

*Article history:*
Received 1 November 2016
Received in revised form 19 January 2017
Accepted 22 January 2017
Corresponding Editor: Eskild Petersen, Aarhus, Denmark

*Keywords:*
Peptide microarray
Bacille Calmette–Guérin
Immuno-editing
Immunoglobulin gamma

SUMMARY

*Background:* Bacille Calmette–Guérin (BCG) is the world's most widely distributed vaccine, used against tuberculosis (TB), in cancer immunotherapy, and in autoimmune diseases due to its immunomodulatory properties. To date, the effect of BCG vaccination on antibody responses to host proteins has not been reported. High-content peptide microarrays (HCPM) offer a unique opportunity to gauge specific humoral immune responses.

*Methods:* The sera of BCG-vaccinated healthy adults were tested on a human HCPM platform (4953 randomly selected epitopes of human proteins) to detect specific immunoglobulin gamma (IgG) responses. Samples were obtained at 56, 112, and 252 days after vaccination. Immunohistology was performed on lymph node tissue from patients with TB lymphadenitis. Results were analysed with a combination of existing and novel statistical methods.

*Results:* IgG recognition of host peptides exhibited a peak at day 56 post BCG vaccination in all study subjects tested, which diminished over time. Primarily, IgG responses exhibited increased reactivity to ion transporters (sodium, calcium channels), cytokine receptors (interleukin 2 receptor β (IL2Rβ), fibroblast growth factor receptor 1 (FGFR1)), other cell surface receptors (inositol, somatostatin, angiopoeitin), ribonucleoprotein, and enzymes (tyrosine kinases, phospholipase) on day 56. There was decreased IgG reactivity to transforming growth factor-beta type 1 receptor (TGFβR1) and, in agreement with the peptide microarray findings, immunohistochemical analysis of TB-infected lymph node samples revealed an overexpression of TGFβR in granulomatous lesions. Moreover, the vesicular monoamine transporter (VMAT2) showed increased reactivity on days 112 and 252, but not on day 56 post-vaccination. IgG to interleukin 4 receptor (IL4R) showed increased reactivity at 112 days post-vaccination, while IgG to IL2Rβ and FGFR1 showed decreased reactivity on days 112 and 252 as compared to day 56 post BCG vaccination.

*Conclusions:* BCG vaccination modifies the host's immune landscape after 56 days, but this imprint changes over time. This may influence the establishment of immunological memory in BCG-vaccinated individuals.



* Correspondence author.
*E-mail addresses:* markus.maeurer@ki.se, markus.maeurer@gmail.com (M. Maeurer).

http://dx.doi.org/10.1016/j.ijid.2017.01.027

**Contents**



## Introduction

*Mycobacterium bovis* bacille Calmette–Guérin (BCG) is the most widely used vaccine in the world, and the only licensed preventive vaccine for tuberculosis (TB), with over four million doses administered since 1921.[1] Although variably effective against pulmonary TB in adults, BCG still provides at least 70% protection against childhood forms of active TB disease in TB endemic countries.[2,3] As a live attenuated vaccine, BCG is a potent inducer of cellular immune responses (mainly CD4 and CD8 T-cells), as well as B-cell-mediated immune responses and antigen-specific antibody production.[4–6] The high degree of genetic and thus antigenic similarity between BCG and *Mycobacterium tuberculosis* forms the basis for its documented although varied effectiveness against childhood TB.[2,7] In addition to TB prevention, the immunostimulatory properties of BCG have also been explored in the treatment of bladder cancer for over 35 years,[4,8] and more recently in type 1 diabetes,[9] as well as in 'clinically isolated syndrome' known as the precursor to multiple sclerosis.[10] One of the most clinically advanced novel TB vaccine candidates, VPM1002, is based on the genetic backbone of BCG,[11,12] and is also being tested therapeutically in patients with non-muscle invasive bladder cancer due to its improved immunogenicity and safety profile compared to the parental BCG vaccine (ClinicalTrials.gov identifier: NCT02371447). These multiple therapeutic characteristics of the BCG vaccine strongly underline its importance from a global healthcare perspective.

Although BCG-induced immune responses have been studied in the context of T- and B-cell reactivity to mycobacterial antigens, they have not been studied in the context of the immune response landscape to host proteins. Molecular mimicry between mycobacterial heat shock protein 65 and human proteins such as lactoferrin, transferrin, and human leukocyte antigen (HLA)-DR-β has been reported in the past,[13] while autoantibody responses to a variety of host proteins, i.e., cardiolipin and RNA polymerase in patients with TB, is well documented and has been reviewed elsewhere.[14] Furthermore, the ability of BCG to modify the host immune response in juvenile patients with type 1 diabetes via killing of autoimmune cells and promoting regeneration of pancreatic islets cells has also been published.[9] Thus, it is plausible to assume that BCG vaccination may leave an imprint on the host's physiology, inducing the recognition of specific host-derived epitopes and influencing the ensuing immune responses.

Among host immune response factors, the transforming growth factor beta (TGF-β) signalling pathway is an important component of cellular regeneration, cell proliferation, vascular reconstruction, and control of adverse immune reactions.[15,16] The TGF-β cytokine binds to a receptor complex comprising TGFβR1 and TGFβR2, which initiates the signalling cascade necessary for the various aforementioned cellular processes and immune regulation. However, premature activation of the TGF-β pathway may potentially hinder the development of meaningful effector immune responses, leading to chronic inflammation and disease. The efficacy of BCG vaccination can be hampered by an increased presence of TGF-β levels,[17] while patients with active TB are known to have high levels of circulating TGF-β and an impaired immune system.[18]

In the current study, a high-content human peptide microarray (HCPM) encompassing over 6000 individual epitopes corresponding to various human proteins was used to determine specific IgG responses induced by BCG vaccination. This platform allows for the detection of antibody responses with high specificity and sensitivity at the epitope level to gauge molecularly defined target reactivity using bioinformatic scripts and available software environments (Bioconductor, R).[37,38] The current report describes the molecular 'landscape' of the overall humoral immune recognition induced by BCG vaccination.

## Materials and methods

### *Serum samples*

This study received ethical approval from the Stockholm South Ethics Committee (diary number 12968). Serum samples were obtained from healthy adult (>18 years) Caucasian individuals with no previous exposure to mycobacteria or BCG vaccination, i.e., tuberculin skin test (TST)-negative study subjects. The serum was prepared from the peripheral blood of five healthy individuals who were vaccinated with the bacille Calmette–Guérin (BCG) vaccine. Samples were obtained at the following time points: day 0 (at vaccination, the time point reflects the serum prior to vaccine

administration; individuals were TST- and Quantiferon-negative); day 56, day 112, and day 252 after vaccination (kindly provided by Dr Daniel Hoft, St. Louis University Medical Centre, USA). Altogether, 20 serum samples were used. All volunteers participated in the study after providing written informed consent.

*Microarray slides and experiments*

Peptide microarray slides were customized and manufactured by JPT (Berlin, Germany). The slides contain three identical sub-arrays with 5776 positions on each sub-array arranged in 16 printing blocks, with spots in each block in a 19 × 19 matrix (a schematic representation of a microarray is available in the **Supplementary Material**, Figure S1). Four thousand five hundred and ninety-one unique, randomly selected peptides were printed across each sub-array (**Supplementary Material**, Table S8). Each sub-array also contains positive and negative controls. In total, considering the three sub-arrays, each microarray contains 17 328 spots: 16 146 of these spots are printed with peptides, 918 contain positive controls and various other controls, and 264 spots are negative controls ('empty spots').

Twenty serum samples (four time points × five volunteers) were processed in individual peptide microarray slides. All volunteers participated in the study after providing written informed consent. A further four slides were prepared using only buffer and secondary antibody, in order to help identify peptides giving a 'false-positive' response (see below).

Experiments were performed based on a standardized protocol.[19] Briefly, 300 µl sera diluted at 1:100 in washing solution (filtered phosphate-buffered saline (PBS), 3% foetal calf serum (FCS; Sigma, Germany), and 0.5% Tween (Sigma, Germany)) were added to the peptide microarray slide and covered with a cover slip (Gene-Frame, Abgene, UK). Diluted sera were distributed evenly over the microarray slide and incubated at 4 °C in a humid chamber for 16 h. After removal of the cover slip, the slides were washed five times on a shaker at room temperature, 5 min per wash (2 × with washing solution, 2 × with sterile water, and 1 × wash with filtered Milli-Q water at the end). Just after the washing procedure, 300 µl of Cy5-labeled polyclonal goat anti-human IgG (affinity-purified secondary antibody, Abcam, UK; product number ab97172), diluted at 1:500 in washing solution, was added to the slides in the dark. The slides were covered with a cover slip and incubated in the dark, in a humidified chamber at room temperature for 1 h. The same washing protocol was repeated after the incubation period with the secondary antibody. Prior to scanning, the slides were dried in a slide spinner (Euro Tech, UK). Five additional slides were processed using only buffer, using the first incubation step of the protocol for detecting false-positive spots due to non-specific binding of the secondary antibody.

High definition images from the slide sub-array were acquired with a GenePix 4000 B microarray scanner (Axon Instruments–Molecular Devices, Union City, USA) using wavelengths of 635 nm (red channel, for the specific IgG signal quantification) and 532 nm (green channel, positive controls for grid alignment and orientation). Data acquisition from the images was performed with the software GenePix 6 Pro (Axon Instruments–Molecular Devices, Union City, USA).

The peptide microarray data analysis was performed according to established protocols[18–22] and novel approaches, as outlined in the sections below.

*Pre-processing of peptide microarray data*

*Quality control*

Electronic images of the sub-array were inspected to ensure that artefacts were not included in the analysis and to detect spots

**Table 1**
Significance analysis of microarrays (SAM) time course analysis results. The peptides with intensity values negatively correlated with time ($q$-value <0.001) are given in green, ranked by absolute SAM score. No statistically stronger recognition of peptides over time was found.

| Peptide | Name | Description | Sc. |
|---|---|---|---|
| MATSEAVMGLGDP | GAB2 (P47870) | Gamma-aminobutyric acid receptor GABA(A) | -1.78 |
| GGIHEDYQLPYYD | TGFBR1 (P36897) | TGF-beta receptor 1 | -1.62 |
| KLATFPNGPSVTL | ADCY3 (O60266) | Adenylate cyclase type 3 | -1.58 |
| KLDSELSRAQEKA | BAI1 (O14514) | Brain-specific angiogenesis inhibitor 1 | -1.47 |
| LAVQAYSHQNNPH | GJC1 (P36383) | Gap junction gamma-1 protein (Connexin-45) | -1.42 |
| EAGESWKSILNSL | RYR2 (Q92736) | Ryanodine receptor 2 | -1.32 |
| IMPLSAAMFQSER | RYR1 (P21817) | Ryanodine receptor 1 | -1.32 |
| KEQSEVGSMGALL | SEC61A1 (P61619) | Protein transport protein Sec61 subunit alpha isoform 1 | -1.21 |
| SLEPQKSLGDEGL | PLCB3 (Q01970) | 1-phosphatidylinositol 4,5-bisphosphate phosphodiesterase beta-3 | -1.21 |
| GNGYSKAGIPQHH | NECTIN1 (Q15223) | Nectin -1 | -1.17 |
| HAKGNLQEYLTRH | TGFBR2 (P37173) | TGF-beta receptor type-2 | -1.17 |
| ELNLKDAISYVAE | SLC9A3 (P48764) | Sodium/hydrogen exchanger 3 | -1.16 |
| FVAESTRDQEATG | CHRNE (Q04844) | Acetylcholine receptor subunit epsilon | -1.16 |
| LDGINRHSFNSFR | ADCY7 (P51828) | Adenylate cyclase type 7 | -1.16 |

erroneously flagged by the software or not identified. Signal intensity values were computed as log2 (foreground/background) ('index' values). Diagnostic plots were created and examined (as in Reilly and Valentini[20]). All spots or areas that did not represent a high quality signal were removed from the analysis. For each slide (representing one patient at one time point), outliers and abnormal values were identified and removed.

*False-positive and 'empty' spot removal, and exclusion of low intensity signal spots*

All spots identified as false-positive on the buffer slides were removed from the analysis.[20]

*Normalization*

The normalization process was performed using the simple linear model, as described previously[20,23]: $I = slide_i + subarray_j + block_k + \varepsilon$, where $I$ is the measured signal intensity; $slide_i$,$subarray_j$, and $block_k$ are the effects on the intensities due to the position of the spot in one of the slides, sub-arrays, and printing blocks, respectively; ε is the residual, which contains the biological interaction, and slide and sub-array interaction ($slide_i$ * $subarray_j$). Data were fitted into the linear model and the estimated slide, sub-array, and block effects removed.

*Analysis and data mining*

First, peptide recognitions were analysed to identify peptide intensities statistically up-regulated or down-regulated over time, using time-course analysis in significance analysis for microarrays (SAM).[24]

Second, a cut-off threshold for recognition was defined as μ + 2 SD, where SD is the standard deviation of μ, the mean intensity value of all negative controls ('empty' spots, i.e., with no peptides printed).[19,21] By using this threshold, two different analyses were performed: (1) the total number of hits, i.e., the peptides above the cut-off (IgG-reactive peptides) at each time point (inclusive recognition analysis, IRA); (2) the number of hits at one time point of the peptides to which no IgG reactivity was observed in the comparison time point (exclusive recognition analysis, ERA). For both the IRA and ERA, top peptides identified in each group were plotted according to the index value and number of recognitions.

Third, peptide differential recognition (the statistical comparison of peptide microarray intensities between two groups) was performed between each couple of time point groups using empirical Bayes methods, from LIMMA packages (linear models for microarray data) in Bioconductor project.[25]

Fourth, a simultaneous comparison of all groups was performed using prediction analysis for microarrays (PAM) multiclass analysis[26] (a robust statistical method based on shrunken centroid classification) in order to simultaneously compare all of the time point groups and to identify which peptides contribute to the variations between the groups and to what extent. The results from PAM were also submitted to a cluster analysis.

Fifth, a new visualization method was proposed. For each individual, using a time-series of scatterplots of normalized index vs. log2 (background), new IgG-reactive peptides were highlighted (in red). Similarly, peptides that no longer exhibited IgG reactivity were also highlighted (in green). This technique makes it possible to visualize the development of the immune response and its importance.

Finally, bulkiness–polarity immune recognition surfaces were created for each individual at the different time points.[27]

All pre-processing and statistical analyses were performed using in-house scripts and open-source packages of Bioconductor, R software (http://www.bioconductor.org).

*Immunohistochemistry*

Frozen lymphoid tissue samples were obtained from Ethiopian patients diagnosed with a local TB lymphadenitis ($n = 5$) or a non-infectious tonsil hyperplasia ($n = 5$) (ethical approval diary numbers 365/00 and 2007/141-32). Lymph nodes and tonsils are lymphoid tissue, although tonsils have a different architecture and arrangement of the germinal centres (GC), as well as size of the follicular dendritic cell network, compared to classical lymph nodes.[28] Nevertheless, the majority of the T-cells that occur in both structures in healthy individuals comprise CD4 T-cells, although most of these T-cells tend to occur at the fringe of the GC in tonsils, whereas they occur closer to the centre in lymph nodes. TB tissue biopsies were collected from the Paediatrics Department, Black Lion University Hospital, Addis Ababa, Ethiopia and control tonsils from the Karolinska University Hospital Huddinge, Sweden, after informed consent was obtained from the patients.

Frozen tissue sections were assessed for the expression of the TGFβR protein with the ABC method using a diaminobenzidine substrate (Vector Laboratories, Burlingame, CA, USA) and haematoxylin for nuclear counterstaining. Briefly, frozen tissues were sectioned (8 μm), mounted, and fixed in 4% paraformaldehyde (Sigma Aldrich AB, Stockholm, Sweden) on HTC slides (Histolabs, Gothenburg, Sweden) before permeabilization in saponin (Sigma Aldrich AB, Stockholm, Sweden). This was followed by overnight incubation at 4 °C with one of the following primary antibodies: a commercially available mouse anti-human monoclonal antibody recognizing the TGFβR2 extracellular domain (clone MM0056-4F14; Abcam, Cambridge, UK) or a custom-made, affinity-purified rabbit anti-human monoclonal antibody specifically recognizing the GKQYWLITAFHAK transmembrane epitope of TGFβR2 (GenScript Biotech, NJ, USA). For protein detection, a biotinylated secondary swine anti-rabbit F(ab′) antibody or a goat anti-mouse IgG antibody was used (Dako, Glostrup, Denmark). Haematoxylin stain was used for nuclear counterstaining. Stained images were analyzed on a DMR-X microscope to determine the percentage positively stained area in the total cell area using the computerized image analysis program Leica QWin 550 (Leica Microsystems, Wetzlar, Germany).

## Results

*Time-dependent IgG-peptide recognition post BCG vaccination*

To map the serum IgG response to human host proteins and to determine the increased and/or decreased immune reactivity, longitudinal analyses of serum samples from five individuals obtained at day 0, 56, 112, and 252 after BCG vaccination were performed on an HCPM containing randomly selected peptides corresponding to human proteins. First, IgG-peptide recognition intensities were studied over time using SAM time course analysis. Each individual's timeline (0, 56, 112, and 252 days) represented one data time course. This analysis assessed the different IgG-peptide recognition patterns that emerge over time (positively or negatively, with a significant $p$-value) (Table 1). Despite the fact that empirically many peptides exhibited increased recognition, the value of many of these IgG responses decreased over time. Only 14 peptides showed a statistically significant trend, albeit with a decreased overall serum IgG reactivity (Table 1).

*Differences in IgG-peptide recognition post BCG vaccination within and between time points*

The lack of strong positive IgG reactivity to host peptides over time could be due to a non-linear trend in the IgG response, i.e., strong IgG responses appearing exclusively at certain time points.

Therefore, IgG-peptide recognition patterns were examined at days 0, 56, 112, and 252 post BCG vaccination, followed by a comparison between the different time points. Peptides with increased IgG reactivity (above the cut-off for recognition) showed a similar visual pattern for all the four time points post-vaccination (**Supplementary Material**, Figure S1). In particular, a positive peptide recognition was constantly present in all five serum samples at day 0 for 236 peptides. Here, the peptide CGRMACSPTHDEH (neuronal acetylcholine receptor subunit alpha-7) emerged with the highest average intensity level, while ranking high also at days 56, 122, and 252 post-vaccination (third, again first, and fifth, respectively).

Similarly, the peptides EHATGEACWWTIH (brain ryanodine receptor 3) and QWWNMPSPSVDPY (striatin 3) had the second and third highest increase in IgG reactivity at day 0, respectively, which also ranked high at the later time points. At 56, 112, and 252 days post BCG vaccination, 273, 256, and 262 peptides, respectively, exhibited an IgG reactivity above the cut-off value in all five individuals.

It was observed that the 'top recognized peptides' exhibiting increased IgG reactivity were conserved over time. Almost all of the top 10 peptides with consistently high average intensity values at a given time point were also found in the top 15 positions at each of the remaining time points. The only time point with a slightly different pattern of IgG-peptide recognition appeared to be at day 56 post-vaccination. The top 15 peptides displaying increased IgG reactivity at each time point post BCG vaccination are provided in the **Supplementary Material** (Table S1).

The cut-off-based comparisons of serum IgG responses carried out by ERA showed that most of the variation occurred between days 0 and 56 post-vaccination (Figure 1). At day 0 post-vaccination, 2434 peptides were found to be never IgG-reactive in any of the samples, of which 9 peptides were always recognized in all five serum samples at day 56 post BCG vaccination. In addition, a further 91 out of the 2434 peptides were recognized in four out of five serum samples. At day 112 post-vaccination, 2 and 10 peptides out of the 2434 peptides never responding at day 0 were IgG-reactive in all five serum samples and in four out of five serum samples, respectively. Moreover, 2 and 9 out of 2434 peptides had IgG-reactivity in five out of five serum samples and four out of five serum samples, respectively, on day 252 post-vaccination, albeit without reactivity on day 0. All ERA results are reported in Figure 1. The top peptide with constantly high serum IgG reactivity at day 56 post-vaccination but not at day 0 was IEMKKRSPISTDT (CIN7, sodium channel protein type 7). The top peptides with increased IgG reactivity from all ERA comparisons are listed based on the number of hits and signal intensity in the **Supplementary Material** (Tables S2–S7).

*Differential IgG-peptide recognition over time: comparison of multiple time points to day 0 post BCG vaccination*

In addition to the peptides identified with ERA comparisons, peptides with statistically significant differential serum IgG reactivity were obtained using LIMMA analysis. The peptides with increased or decreased IgG reactivity, with an absolute log fold-change value higher than 0.58 (corresponding to a fold-change of $\pm 1.5$) are reported in Tables 2–4 . When IgG reactivity at day 56 post-vaccination was compared to that at day 0, differential reactivity to 115 peptides was identified (44 peptides with increased reactivity, 71 peptides with decreased reactivity; $q$-value $\leq 0.05$). Some of the peptides with increased reactivity in this comparison included APEALFDRIYTHQ (fibroblast growth factor receptor 1, FGFR1), KVLKCNTPDPSKF (interleukin-2 receptor beta, IL2Rβ), NHLKSKEVWKALLQE (60 kDa SS-A/Ro ribonucleoprotein), and ADYINANYIDGYH (mast/stem cell growth factor receptor Kit)

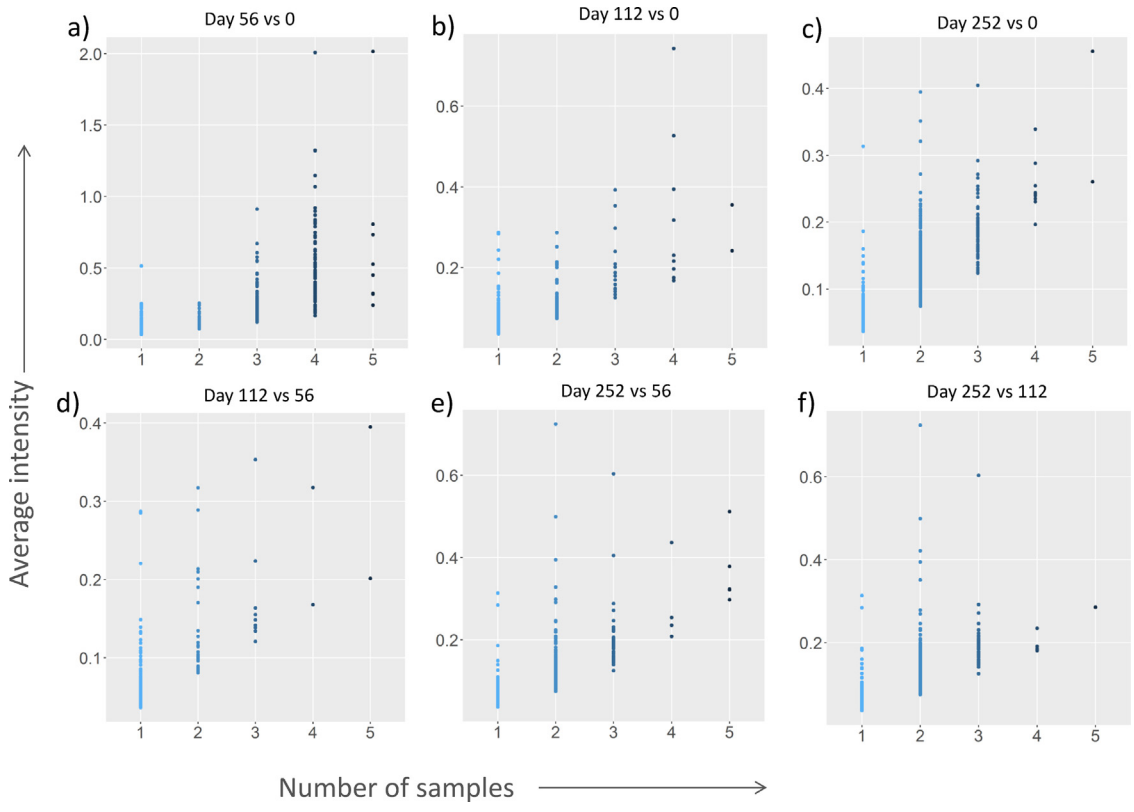


**Figure 1.** Number of peptides without IgG reactivity in the reference group by the number of hits and by average intensity in the comparison group. Shown are the comparisons for (a) day 56 vs. day 0; (b) day 112 vs. day 0; (c) day 252 vs. day 0; (d) day 112 vs. day 56; (e) day 252 vs. day 56; (f) day 252 vs. day 112.

**Table 2**
LIMMA differential recognition analysis results for samples at day 56 vs. samples at day 0. Top selected peptides: peptides with increased IgG reactivity are given in red; peptides with decreased IgG reactivity are given in green (absolute log fold-change ≤0.58 corresponding to ±1.5 times).

| Peptide | FC | Name | Description |
|---|---|---|---|
| GVQIAKGMYYLEE | 6.92 | ERBB3 (P21860) | Receptor tyrosine-protein kinase erbB-3 |
| YIQGAASPKDMLI | 4.48 | CACNA2D1 (P54289) | Voltage-dependent calcium channel subunit alpha-2/delta-1 |
| IEMKKRSPISTDT | 4.23 | SCN7A (Q01118) | Sodium channel protein type 7 subunit alpha |
| CAFRSQLETPETL | 3.07 | TNFRSF1B (P20333) | Tumor necrosis factor receptor superfamily member 1B |
| VKDPTEYTGPESY | 2.57 | ITPR2 (Q14571) | Inositol 1,4,5-trisphosphate receptor type 2 |
| ATYRRPSVAKLIN | 2.48 | SSTR4 (P31391) | Somatostatin receptor type 4 (SS-4-R) |
| APEALFDRIYTHQ | 2.45 | FGFR1 (P11362) | Fibroblast growth factor receptor 1 |
| DVVRTMSTEQARS | 2.13 | TAF1 (P21675) | Transcription initiation factor TFIID subunit 1 |
| TEHSMLSADEDSP | 2.06 | NRF1 (Q16656) | Nuclear respiratory factor 1 |
| ELHRQWELLLEKMRE | 1.99 | SPTAN1 (Q13813) | Spectrin alpha chain, non-erythrocytic 1 |
| LLHGYAFSQDENG | 1.84 | ATP8A1 (Q9Y2Q0) | Phospholipid-transporting ATPase IA |
| HFWSTLSPIAPRS | 1.83 | ELK1 (P19419) | ETS domain-containing protein Elk-1 |
| YIDPFTYEDPNEA | 1.78 | EPHB1 (P54762) | Ephrin type-B receptor 1 (ELK1) |
| LFSGSLRMNLDPF | 1.75 | ABCC2 (Q92887) | Canalicular multispec organic anion transporter 1 |
| QRDAEELEKWIQEKL | 1.74 | SPTAN1 (Q13813) | Spectrin alpha chain, non-erythrocytic 1 |
| PGDYSTTPGGTLF | 1.74 | EIF4EBP1 (Q13541) | Eukaryotic translation initiation factor 4E-binding protein 1 |
| NTSYPLSPLSDFA | 1.72 | PLA2G4A (P47712) | Cytosolic phospholipase A2 (cPLA2) |
| LLMYLRQCSGPKE | 1.7 | ADAM21 (Q9UKJ8) | Disintegrin/metalloprot domain p21 |
| DDLADQTAIEYGT | 1.7 | GRIK4 (Q16099) | Glutamate receptor ionotropic, kainate 4 (GluK4) |
| KVLKCNTPDPSKF | 1.68 | IL2RB (P14784) | Interleukin-2 receptor beta |
| KKPGKESPWEVLK | **1.63** | HRH1 (P35367) | Histamine H1 receptor |
| DEEGYMTPMRDKP | 1.6 | ERBB4 (Q15303) | Receptor tyrosine-protein kinase erbB-4 |
| PTPDATTPQAKGF | 1.55 | TY3H (P07101) | Tyrosine 3-monooxygenase |
| KQSPSSSPTRERS | 1.54 | PCYT1A (P49585) | Choline-phosphate cytidylyltransferase A |
| KGKEKDSPFKPKL | 1.54 | RBBP5 (Q15291) | Retinoblastoma-binding protein 5 |
| CGMTCAELYEKLP | 1.52 | TEK (Q02763) | Angiopoietin-1 receptor |
| NHLKSKEVWKALLQE | 1.52 | TROVE2 (P10155) | 60 kDa SS-A/Ro ribonucleoprotein |
| AFLRSGSVYEPLK | 1.52 | PHKB (Q93100) | Phosphorylase b kinase regulatory subunit beta |
| ADYINANYIDGYH | 1.51 | PTPRU (Q92729) | Mast/stem cell growth factor receptor Kit |
| SPEKAKSPAKEEA | 0.66 | NEFH (P12036) | Neurofilament heavy polypeptide (NF-H) |
| HQDRIDGVTIQARQF | 0.66 | SPTAN1 (Q13813) | Spectrin alpha chain, non-erythrocytic 1 |
| LYTLFDAIIGSHD | 0.66 | GUCY2D (Q02846) | Retinal guanylyl cyclase 1 (RETGC-1) |
| KMLKEGATASEYK | 0.66 | FLT1 (P17948) | Vascular endothelial growth factor receptor 1 (VEGFR1) |
| GLALQRQGKLFGAAE | 0.65 | SPTAN1 (Q13813) | Spectrin alpha chain, non-erythrocytic 1 |
| ITRPSQRPKTPPT | 0.65 | KIR3DL3 (Q8N743) | Killer cell immunoglobulin-like receptor 3DL3 |
| KNIEKPSGTDPAG | 0.65 | DCC (P43146) | Netrin receptor DCC Colorectal cancer suppr |
| MEPGFREVSFYYS | 0.65 | IGF1R (P08069) | Insulin-like growth factor 1 receptor |
| GVDPSTGKVQLTR | 0.65 | SYT11 (Q9BT88) | Synaptotagmin-11 |
| GVITIESQVHPQS | 0.64 | ITGB4 (P16144) | Integrin beta-4 |
| TPVVSVTTPSLPP | 0.64 | MEF2A (Q02078) | Myocyte-specific enhancer factor 2A |
| KEAGHGTTKEEIT | 0.63 | ATP2B4 (P23634) | Plasma membrane calcium-transporting ATPase 4 |
| KKESQPGSGAVEM | 0.63 | AQP6 (Q13520) | Aquaporin-6 (AQP-6) (Aquaporin-2-like) |
| GPCGSLKAPSPRS | 0.62 | HCRTR1 (O43613) | Orexin receptor type 1 (Ox-1-R) (Ox1-R) |
| LRSGPFYLEGLDL | 0.62 | NPR2 (P20594) | Atrial natriuretic peptide receptor 2 |
| LANTVEAGVESSQ | 0.61 | RYR1 (P21817) | Ryanodine receptor 1 |
| LARQTASVAPKEE | 0.6 | SLC5A5 (Q92911) | Sodium/iodide cotransporter Na(+)/I(-) cotransp |
| EEELIKTKQDEVNAA | 0.6 | SPTAN1 (Q13813) | Spectrin alpha chain, non-erythrocytic 1 |
| IPSENKENSAVPV | 0.6 | SCN3B (Q9NY72) | Sodium channel subunit beta-3 |
| IAVSSIQKAKGYQ | 0.58 | GJA8 (P48165) | Gap junction alpha-8 protein |

**Table 3**
LIMMA differential recognition analysis results for samples at day 112 vs. samples at day 0. Top selected peptides: peptides with increased IgG reactivity are given in red, peptides with decreased IgG reactivity are given in green (absolute log fold-change ≤0.58 corresponding to ±1.5 times).

| Peptide | FC | Name | Description |
|---|---|---|---|
| VDLRHVSVYGSVY | 1.51 | VMAT2 (Q05940) | Synaptic vesicular monoamine transporter |
| GGIHEDYQLPYYD | 0.47 | TGR1 (P36897) | Transforming growth factor beta receptor type 1 |

**Table 4**
LIMMA differential recognition analysis results for samples at day 252 vs. samples at day 0. Top selected peptides: peptides with increased IgG reactivity are given in red, peptides with decreased IgG reactivity are given in green (absolute log fold-change ≤0.58 corresponding to ±1.5 times).

| Peptide | FC | Name | Description |
|---|---|---|---|
| VDLRHVSVYGSVY | 1.7 | VMAT2 (Q05940) | Synaptic vesicular monoamine transporter |
| GGIHEDYQLPYYD | 0.35 | TGR1 (P36897) | Transforming growth factor beta receptor type 1 |

(Table 2). The number of differentially recognized peptides decreased to five (one peptide with increased reactivity, four peptides with decreased reactivity) and two peptides only (one peptide with increased reactivity, one peptide with decreased reactivity) at day 112 and day 252 post-vaccination compared to day 0, respectively (all $q$-values ≤0.05). GGIHEDYQLPYYD (TGFβR1) exhibited decreased IgG reactivity on days 112 and 252 post-vaccination vs. day 0, while VDLRHVSVYGSVY (synaptic vesicular monoamine transporter, VMAT2) showed increased reactivity (Tables 3 and 4).

*Differential IgG-peptide recognition over time: comparison of multiple time points to day 56 post BCG vaccination*

IgG-peptide reactivity in serum samples obtained at day 112 and day 252 post BCG vaccination was also compared to day 56 post-vaccination. Peptides with an absolute fold-change of serum IgG reactivity higher than 1.5 are reported in Tables 5 and 6. At day 112 post BCG vaccination, 146 peptides displayed differential IgG reactivity (66 peptides with increased reactivity, 80 peptides with decreased reactivity), while 39 peptides had differential reactivity at day 252 post-vaccination (18 peptides with increased reactivity, 21 peptides with decreased reactivity). VDLRHVSVYGSVY (synaptic vesicular monoamine transporter) showed increased reactivity, while KVLKCNTPDPSKF (IL2Rβ) showed decreased reactivity at day 112 and day 252 compared to day 56 post-vaccination, respectively. No major differences were observed on comparison of IgG reactivity at day 252 to day 112 post-vaccination, with the exception of one peptide that had decreased reactivity at a low fold-change (ITTLAKDTPLEEV (chloride channel Kb), fold-change 0.68, i.e., −0.56 times).

*Identification of predictive peptides for the simultaneous characterization of the IgG reactivity at the various time points*

PAM multiclass comparison identified 145 peptides with statistically significant IgG reactivity, which characterized the various time points. The 20 top-ranked peptides are reported in Table 7. A visualization of comparative differences in serum IgG reactivity to peptides (Figure 2) represents the contribution of the predicted peptides for each time point post-vaccination. A peptide intensity plot for each serum sample and time point post-vaccination is illustrated in Figure 3. An unsupervised cluster analysis of the identified peptides was also performed (heat map reported in the **Supplementary Material**, Figure S3).

*Visualization of individual changes in peptide responses and in immune recognition profiles*

The variations in peptide intensities over time for each individual were assessed by plotting the data using a new visualization technique, whereby the new IgG-reactive peptides (above the recognition cut-off) at each time point post-vaccination, as well as the peptides that are no longer IgG-reactive, are marked with a different symbol and colour. As a paradigm, the scatterplots of IgG reactivity intensities vs. log backgrounds for all four time points post-vaccination for individual 1 are reported in Figure 4 (plots for individuals 2–5 are reported in the **Supplementary Material**, Figures S4–S7). In agreement with the previous analyses reported in this study, the increase in serum IgG reactivity peaked at day 56 post-vaccination and waned at day 112 and day 252 post-vaccination). However, several new IgG-reactive peptides were still present at day 112 and day 252 post-vaccination, particularly for individual 5 (**Supplementary Material**, Figure S7). Finally, three-dimensional immune recognition surfaces were created for the average IgG reactivity intensities at all four time points post-vaccination in order to estimate the peptide recognition profile and the time-dependent landscape (Figure 5). These analyses illustrated the dynamic nature of the immune-recognition IgG profile of the host protein over time (see also the **Supplementary Material**, movie file *'bcg'*).

*Expression and distribution of TGFβR2 in TB lymph node tissue*

The results from the peptide microarray suggest that there is a decreased IgG reactivity to the TGFβR1. Since TGF-β is an important signalling pathway in cellular physiology, as well as immune responses,[15,16] TGFβR protein expression in lymph node tissue obtained from patients with local TB lymphadenitis was assessed using immunohistochemistry. For this purpose, a monoclonal antibody recognizing the TGFβR2 transmembrane epitope GKQYWLITAFHAK, as well as a commercially available anti-human TGFβR2 antibody, was tested. TGFβR1 and TGFβR2 have similar ligand-binding affinities and both also have a high affinity for TGF-β1 and low affinity for TGF-β2. TGFβR2 expression was clearly elevated in TB lymph nodes compared to lymphoid tonsil tissue obtained from healthy individuals (Figure 6). TGFβR2 expression was particularly high in the TB granulomas where *M. tuberculosis*-infected macrophages had accumulated.[29] Both tested antibodies resulted in significant TGFβR2 staining in TB lymph nodes; however, the commercial

**Table 5**
LIMMA differential recognition analysis results for samples at day 112 vs. samples at day 56. Top selected peptides: peptides with increased IgG reactivity are given in red, peptides with decreased IgG reactivity are given in green (absolute log fold-change ≤0.58 corresponding to ±1.5 times). Peptides with IgG reactivity also found in the exclusive recognition analysis (ERA) top 20 are given in bold.

| Peptide | FC | Name | Description |
|---|---|---|---|
| **LAETTEDFWRMLW** | 3.09 | PTPRS (Q13332) | Receptor-type tyrosine-protein phosphatase S |
| **DLFSYGFDGLHLW** | 1.77 | RYR2 (Q92736) | Ryanodine receptor 2 |
| **VDLRHVSVYGSVY** | 1.76 | VMAT2 (Q05940) | Synaptic vesicular monoamine transporter |
| **LAVSFFSERKYFW** | 1.71 | VIPR1 (P32241) | Vasoactive intestinal polypeptide receptor 1 |
| **IAVSSIQKAKGYQ** | 1.68 | GJA8 (P48165) | Gap junction alpha-8 protein |
| **MSSSEEVSWISWF** | 1.67 | CSNK2B-LY6G5B-696 (N0E4D3) | Protein kinase regulator |
| **LDREPPRSPQSSH** | 1.66 | IL4R (P24394) | Interleukin-4 receptor subunit alpha |
| **KEPMVARKQKLADSL** | 1.61 | SPTAN1 (Q13813) | Spectrin alpha chain, non-erythrocytic 1 |
| **MKVRKSSTPEEVK** | 1.61 | CFL1 (P23528) | Cofilin-1 |
| **LATALASDPIPNP** | 1.59 | TNFRSF1A (P19438) | Tumor necrosis factor receptor superfamily member 1A |
| **DDEMTGYVATRWY** | 1.51 | MAPK14 (Q16539) | Mitogen-activated protein kinase 14 |
| **ATRGQTPYPGVEN** | 0.66 | UFO (P30530) | Tyrosine-protein kinase receptor UFO |
| **IGLQMGSNRGASQ** | 0.66 | TAGL (Q01995) | Transgelin |
| **KGKEKDSPFKPKL** | 0.66 | RBB5 (Q15291) | Retinoblastoma-binding protein 5 |
| **QYGGLNSGRPVTP** | 0.66 | PP1B (P62140) | Serine/threonine-protein phosphatase PP1-beta catalytic subunit |
| **AFLRSGSVYEPLK** | 0.66 | PHKB (Q93100) | Phosphorylase b kinase regulatory subunit beta |
| **NGHITTTPTPTQF** | 0.65 | JUN (P05412) | Transcription factor AP-1 |
| **LKEGATHSEHRAL** | 0.65 | VGR2 (P35968) | Vascular endothelial growth factor receptor 2 |
| **CGMTCAELYEKLP** | 0.65 | TEK (Q02763) | Angiopoietin-1 receptor |
| **SDSIPPSKKEILR** | 0.65 | PHOS (P20941) | Phosducin (PHD) MEKA |
| **GDEDFSSIADMDF** | 0.63 | TF65 (Q04206) | Transcription factor p65 |
| **DEEGYMTPMRDKP** | 0.63 | ERBB4 (Q15303) | Receptor tyrosine-protein kinase erbB-4 |
| **NTSYPLSPLSDFA** | 0.63 | PA4A (P47712) | Cytosolic phospholipase A2 (cPLA2) |
| **ADYINANYIDGYH** | 0.61 | PTPU (Q92729) | Receptor-type tyrosine-protein phosphatase U |
| **IKLYGACSQDGPL** | 0.61 | RET (P07949) | Proto-oncogene tyrosine-protein kinase receptor Ret |
| **YIDPFTYEDPNEA** | 0.61 | EPB1 (P54762) | Ephrin type-B receptor 1 (EC 2.7.10.1) (ELK) |
| **GFGHRLSPEYKQN** | 0.61 | GJB1 (P08034) | Gap junction beta-1 protein (Connexin-32) |
| **FYTATEGQYQQQP** | 0.6 | LYN (P07948) | Tyrosine-protein kinase Lyn |
| **KMPLKLLTNHYEQ** | 0.59 | RYR3 (Q15413) | Ryanodine receptor 3 (RYR-3) (RyR3) Brain R |
| **SGVRQVSEDVRSP** | 0.58 | TY3H (P07101) | Tyrosine 3-monooxygenase |
| **QRDAEELEKWIQEKL** | 0.55 | SPTAN1 (Q13813) | Spectrin alpha chain, non-erythrocytic 1 |
| **LFSGSLRMNLDPF** | 0.54 | ABCC2 (Q92887) | Canalicular multispec.organic anion transporter |
| **PGDYSTTPGGTLF** | 0.54 | EIF4EBP1 (Q13541) | Eukaryotic translation initiation factor 4E-binding |
| **MSSHGNSLFLRES** | 0.54 | SLC1A6 (P48664) | Excitatory amino acid transporter 4 |
| **LLHGYAFSQDENG** | 0.54 | ATP8A1 (Q9Y2Q0) | Phospholipid-transporting ATPase IA |
| **FRHDSGYEVHHQK** | 0.54 | APP (P05067) | Amyloid beta A4 protein |
| **GGVHEEYQLPYYD** | 0.52 | ACVR1B (P36896) | Activin receptor type-1B (EC 2.7.11.30) |
| **ALQGFNSPGMLSL** | 0.52 | MEF2A (Q02078) | Myocyte-specific enhancer factor 2A |
| **PDCYSTTPGGTLY** | 0.51 | EIF4EBP3 (O60516) | Eukaryotic translation initiation factor 4E-binding protein 3 |
| **KVLKCNTPDPSKF** | 0.5 | IL2B (P14784) | Interleukin-2 receptor beta |
| **AELYGSDPREELL** | 0.5 | CDH5 (P33151) | Cadherin-5 (7B4 antig.) (Vascular endoth adherin) |
| **AQDTYLVLDKWLL** | 0.5 | EPOR (P19235) | Erythropoietin receptor |
| **DVVRTMSTEQARS** | 0.48 | TAF1 (P21675) | Transcription initiation factor TFIID subunit 1 |
| **QKLADSLRLQQLFRD** | 0.46 | SPTAN1 (Q13813) | Spectrin alpha chain, non-erythrocytic 1 |
| **LSEETPYSYPTGN** | 0.45 | PXN (P49023) | Paxillin |
| **LVTQLMPYGCLLD** | 0.43 | ERBB2 (P04626) | Receptor tyrosine-protein kinase erbB-2 |
| **ATYRRPSVAKLIN** | 0.39 | SSTR4 (P31391) | Somatostatin receptor type 4(SS4R) |
| **APEALFDRIYTHQ** | 0.38 | FGFR1 (P11362) | Fibroblast growth factor receptor 1 |
| **VKDPTEYTGPESY** | 0.37 | ITPR2 (Q14571) | Inositol 1,4,5-trisphosphate receptor type 2 IP3R |
| **KPLAPNPSFSPTP** | 0.35 | TNFRSF1A (P19438) | Tumor necrosis factor receptor superfamily member 1A |
| **HMLKGISIYPETL** | 0.35 | SYT11 (Q9BT88) | Synaptotagmin-11 |
| **CAFRSQLETPETL** | 0.31 | TNFRSF1B (P20333) | Tumor necrosis factor receptor superfamily member 1B |
| **IEMKKRSPISTDT** | 0.26 | SCN7A (Q01118) | Sodium channel protein type 7 subunit alpha |
| **YIQGAASPKDMLI** | 0.24 | CACNA2D1 (P54289) | Voltage-dependent calcium channel subunit alpha-2/delta-1 |

**Table 6**
LIMMA differential recognition analysis results for samples at day 252 vs. samples at day 56. Top selected peptides: peptides with increased IgG reactivity are given in red, peptides with decreased IgG reactivity are given in green (absolute log fold-change ≤0.58 corresponding to ±1.5 times).

| Peptide | FC | Name | Description |
|---|---|---|---|
| VDLRHVSVYGSVY | 1.99 | VMAT2 (Q05940) | Synaptic vesicular monoamine transporter |
| IAVSSIQKAKGYQ | 1.96 | GJA8 (P48165) | Gap junction alpha-8 protein |
| MSSSEEVSWISWF | 1.94 | CSNK2B-LY6G5B-696 (N0E4D3) | Protein kinase regulator |
| KEPMVARKQKLADSL | 1.78 | SPTAN1 (Q13813) | Spectrin alpha chain, non-erythrocytic 1 |
| VYSTDYYRVGGHT | 1.77 | NTRK2 (Q16620) | BDNF/NT-3 growth factors receptor |
| GEPNVSYICSRYY | 1.72 | GSK3B (P49841) | Glycogen synthase kinase-3 beta |
| TGFLTEYVATRWY | 1.66 | MAPK1 (P28482) | Mitogen-activated protein kinase 1 |
| MKVRKSSTPEEVK | 1.62 | CFL1 (P23528) | Cofilin-1 |
| AESWMREKEPIVGST | 1.61 | SPTAN1 (Q13813) | Spectrin alpha chain, non-erythrocytic 1 |
| LDQYKFCYEVALE | 1.55 | PTPRM (P28827) | Receptor-type tyrosine-protein phosphatase mu |
| GGEGPSATANGGL | 1.54 | SELPLG (Q14242) | P-selectin glycoprotein ligand 1 |
| EKKKKTTTIAVEV | 1.5 | HDLBP (Q00341) | Vigilin |
| LGSPLSSPVFPRA | 0.65 | DES (P17661) | Desmin |
| RKVGPGYLGSGGS | 0.65 | RET (P07949) | Proto-oncogene tyrosine-protein kinase receptor Ret |
| FYTATEGQYQQQP | 0.63 | LYN (P07948) | Tyrosine-protein kinase Lyn |
| HKSTPLLIHCRDG | 0.63 | PTPRC (P08575) | Receptor-type tyrosine-protein phosphatase C |
| PTPDATTPQAKGF | 0.61 | TY3H (P07101) | Tyrosine 3-monooxygenase |
| NHLKSKEVWKALLQE | 0.6 | TROVE2 (P10155) | 60 kDa SS-A/Ro ribonucleoprotein |
| IKLYGACSQDGPL | 0.59 | RET (P07949) | Proto-oncogene tyrosine-protein kinase receptor Ret |
| ADYINANYIDGYH | 0.58 | PTPRU (Q92729) | Mast/stem cell growth factor receptor Kit |
| LFSGSLRMNLDPF | 0.55 | ABCC2 (Q92887) | Canalicular multispecific organic anion transp |
| KVLKCNTPDPSKF | 0.54 | IL2RB (P14784) | Interleukin-2 receptor beta |
| MSSHGNSLFLRES | 0.46 | SLC1A6 (P48664) | Excitatory amino acid transporter 4 |
| AGTQRYMAPELLD | 0.41 | AMHR2 (Q16671) | Anti-Muellerian hormone type-2 receptor |
| HMPMSMNELSNPC | 0.34 | ADGRB3 (O60242) | Adhesion G protein-coupled receptor B3 |
| APEALFDRIYTHQ | 0.32 | FGFR1 (P11362) | Fibroblast growth factor receptor 1 |

TGF-β2 antibody showed relatively higher background in healthy control tissue (Figure 6).

## Discussion

The BCG vaccine is widely accepted as a potent inducer of cellular immune responses in humans (CD4 (Th1, Th2, Th17) and CD8 (cytotoxic lymphocytes) T-cells), with a broad specificity, and directed to a range of mycobacterial antigens.[5,30–33] Likewise, antigen-specific CD4+ T-cells that are induced after intravesical BCG instillation therapy in patients with bladder cancer, show similar Th1 cytokine profiles as demonstrated in active TB infection.[34] Using a human HCPM platform, it has been shown for the first time in the present study that BCG vaccination of healthy human adults modifies the IgG response to host targets, with implications for shaping T-cell responses. To the best of the authors' knowledge, this is also the first study to describe the general outcome of BCG vaccination in healthy adults, assessing antibody responses to a broad range of host proteins and not in response to mycobacterial antigens, i.e., anti-BCG/*M. tuberculosis* responses.

BCG-driven modulation of antibody responses to host epitopes was visualized over a 252-day period in vaccinated healthy adults. The peak of differential serum IgG reactivity appearing at 56 days post-vaccination, which waned over time, indicates that BCG vaccination does not leave a permanent imprint on the host's immune profile. Host epitopes belonging to ion transporters (sodium, potassium voltage-gated channels) exhibited the highest increase in reactivity, suggesting that these proteins may have a general effect on immune cell activity and proliferation after BCG vaccination.[35] Increased IgG reactivity to IL2Rβ at day 56 post-vaccination is particularly interesting due to its indispensable role in IL-2 as well as IL-15-mediated signalling, which is central to T-cell activation and proliferation.[36,37] This indicates that BCG may modify the growth factor (IL2, IL-15) responsiveness of T-cells early after vaccination. Additionally, increased serum IgG responses towards other growth factors including FGFR1 and stem cell growth factor receptor 1 (SCFR1, c-Kit), both of which promote T-cell activation and development,[38,39] suggest that a transient interruption in the activation of T-cell responses may be expected within the first 2 months of BCG vaccination. The Ro ribonucleoprotein (Ro-RNP), which is involved in maintaining RNA stability and DNA replication,[40] also showed increased IgG reactivity. Anti-RNP autoantibodies are clinically implicated in the pathogenesis of several autoimmune diseases, i.e., systemic lupus erythematosus, primary biliary cirrhosis, and Sjögren's syndrome,[41,42] although no clear link exists between T-cell function and Ro-RNP responses. Evidently,

**Table 7**
Prediction analysis for microarrays (PAM) multiclass comparison results. Top 20 peptides and their relative scores for each time point: increased IgG reactivity in red, decreased IgG reactivity in green.

| peptide | Name | Description | T0 sc. | T56 sc. | T112 sc. | T252 sc. |
|---|---|---|---|---|---|---|
| **APEALFDRIYTHQ** | FGFR1 (P11362) | Fibroblast growth factor receptor 1 | 0 | 1.07 | 0 | -0.12 |
| **IEMKKRSPISTDT** | SCN7A (Q01118) | Sodium channel protein type 7 subunit alpha | 0 | 1.02 | 0 | 0 |
| **CAFRSQLETPETL** | TNFRSF1B (P20333) | Tumor necrosis factor receptor superfamily member 1B | 0 | 0.83 | 0 | 0 |
| **YIQGAASPKDMLI** | CACNA2D1 (P54289) | Voltage-dependent calcium channel subunit alpha-2/delta-1 | 0 | 0.76 | 0 | 0 |
| **VKDPTEYTGPESY** | ITPR2 (Q14571) | Inositol 1,4,5-trisphosphate receptor type 2 (IP3R 2) (InsP3R2) | 0 | 0.72 | 0 | 0 |
| **GGIHEDYQLPYYD** | TGFBR1 (P36897) | TGF-beta receptor type-1 | 0.72 | 0 | 0 | -0.37 |
| **ATYRRPSVAKLIN** | SSTR4 (P31391) | Somatostatin receptor type 4 (SS4R) | 0 | 0.7 | 0 | 0 |
| **IAVSSIQKAKGYQ** | GJA8 (P48165) | Gap junction alpha-8 protein | 0 | -0.69 | 0 | 0 |
| **LFSGSLRMNLDPF** | ABCC2 (Q92887) | Canalicular multispecific organic anion transporter 1 | 0 | 0.67 | 0 | 0 |
| **GVQIAKGMYYLEE** | ERBB3 (P21860) | Receptor tyrosine-protein kinase erbB-3 | 0 | 0.66 | 0 | 0 |
| **KPLAPNPSFSPTP** | TNFRSF1A (P19438) | Tumor necrosis factor receptor superfamily member 1A | 0 | 0.65 | 0 | 0 |
| **HMLKGISIYPETL** | SYT11 (Q9BT88) | Synaptotagmin-11 | 0 | 0.62 | 0 | 0 |
| **KVLKCNTPDPSKF** | IL2RB (P14784) | Interleukin-2 receptor beta | 0 | 0.59 | 0 | 0 |
| **FYVTKYRQEILTA** | PLXNA3 (P51805) | Plexin-A3 | 0 | 0.55 | 0 | 0 |
| **LVTQLMPYGCLLD** | ERBB2 (P04626) | Receptor tyrosine-protein kinase erbB-2 | 0 | 0.54 | 0 | 0 |
| **QKLADSLRLQQLFRD** | SPTAN1 (Q13813) | Spectrin alpha chain, non-erythrocytic 1 | 0 | 0.51 | 0 | 0 |
| **AQDTYLVLDKWLL** | EPOR (P19235) | Erythropoietin receptor | 0 | 0.49 | 0 | 0 |
| **ADYINANYIDGYH** | PTPRU (Q92729) | Mast/stem cell growth factor receptor Kit (SCFR) | 0 | 0.49 | 0 | 0 |
| **DVVRTMSTEQARS** | TAF1 (P21675) | Transcription initiation factor TFIID subunit 1 | 0 | 0.48 | 0 | 0 |
| **HMPMSMNELSNPC** | ADGRB3 (O60242) | Adhesion G protein-coupled receptor B3 | 0 | 0.46 | 0 | 0 |

the functional impact and subsequent clinical relevance of these epitope-reactive IgG antibodies needs to be further addressed in other studies.

This study found that there was minimal differential IgG-peptide recognition at days 112 and 252 post BCG vaccination compared to baseline (day 0). The comparison of day 112 versus day 0 and of day 252 versus day 0 revealed decreased IgG reactivity to GGIHEDYQLPYYD, which belongs to the transmembrane component of TGFβR1. This suggests that the TGF-β pathway may play a role in BCG-mediated immunomodulation. As mentioned previously, TGF-β signalling is essential for various cellular processes, i.e., cell proliferation, cell cycle arrest, apoptosis, and immunosuppression.[15] Regulatory T-cells and mesenchymal stromal cells neutralize exaggerated inflammation to abate autoimmunity and severe organ damage via TGF-β production.[15,16] However, up-regulation of TGFβR expression in chronic infections such as active TB may prevent imperative T-cell responses and instead promote an immunosuppressive environment in the TB granuloma, which is the major site of bacterial replication. An enhanced tissue expression of both TGF-β and the TGFβR is in line with the previously reported role of TGF-β overexpression in progressive TB disease.[29,43,44]

BCG vaccination could also result in BCG-mediated apoptosis or necrosis of host cells that together with other inflammatory responses may lead to exposure of intracellular proteins to the immune system. Also of note is the increased IgG reactivity to VDLRHVSVYGSVY, which belongs to the transmembrane domain of VMAT2, at day 112 and day 252 post BCG vaccination compared to baseline (day 0), as well as at day 56 post-vaccination. VMAT2 is important for the vesicular release of gamma-aminobutyric acid (GABA) and the transport of neurotransmitters in general.[45,46] Pharmacological inhibitors targeting VMAT2 are in clinical trials for the treatment of attention-deficit/hyperactivity disorder, hypertension, and movement disorders.[47] Antibody responses against VMAT2 may therefore be clinically beneficial in preventing the development of neurological conditions and high blood pressure.

BCG vaccination may also negatively modulate the late Th2 response, as suggested by the increased IgG reactivity to IL-4 receptor alpha subunit (IL4Rα) by serum IgG on day 112 compared to 56 days post BCG vaccination. BCG-triggered humoral immune responses may not necessarily need T-helper cell assistance, since B-cells can engulf mycobacteria on their own and subsequently produce antibodies.[48] Although not necessarily the primary antigen-presenting cell in mycobacteria-directed immune responses, B-cell involvement in orchestrating local and systemic immune-modulation in human pulmonary TB has been documented and reviewed.[49,50] In contrast, T-cell homeostasis and activation is potentially unperturbed in the long-term, since IL2Rβ and FGFR1 exhibited decreased IgG reactivity on days 112 and 252 post BCG vaccination compared to day 56 after vaccination. Decreased IgG reactivity to c-Kit on day 252 may serve as an indicator of focused cellular immune responses, as observed in *M. tuberculosis*-specific precursor-like CD8 T-cells from patients with TB with an HLA-A*02:01 background.[51]

Administering BCG as a means to induce immunomodulatory effects with potential clinical benefit seems plausible based on the differential recognition of cytokine receptors across 252 days after vaccination. The disease-modifying effects observed in patients with non-invasive bladder cancer, type 1 diabetes, or multiple sclerosis after BCG vaccination further attests to this.[9,10,32] Additionally, BCG vaccination of infants in low-income countries has been shown to protect against death from non-TB infections, i.e., sepsis, trypanosomiasis, and diphtheria, by improving the early immune response to the relevant pathogens.[30] An equilibrium between precise and protective versus uncontrolled and destructive inflammatory responses benefits the host.[52] The current study suggests that BCG vaccination modifies the immunological and non-immunological landscape in the host, which may influence

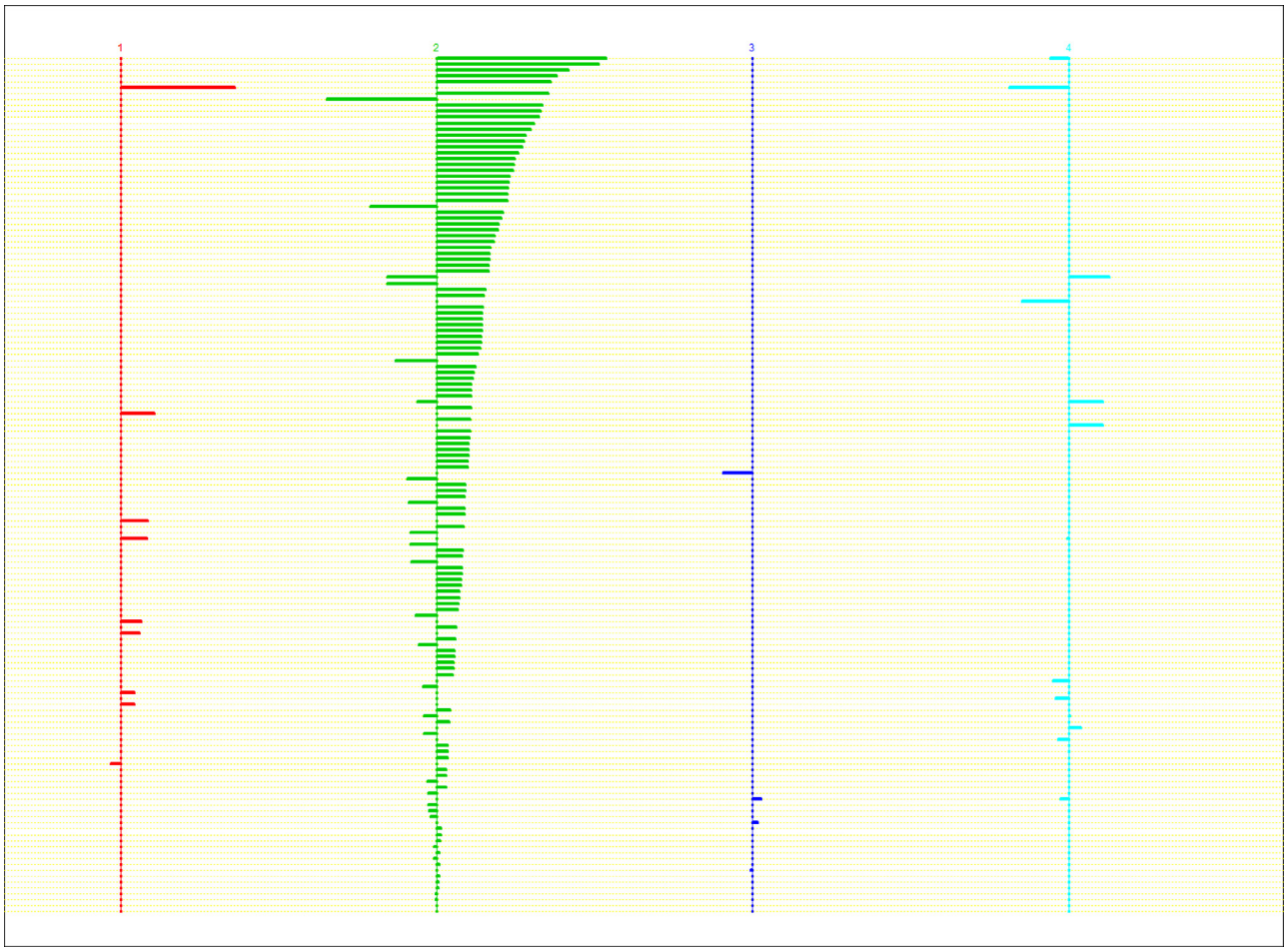


**Figure 2.** Prediction analysis for microarrays (PAM) multiclass centroids plot. Shown is the ranked list of all 145 predictive peptides identified. The length of the horizontal bar is determined as the difference between the overall centroid and the class-specific one (for details, see Valentini et al.[21]), and is representative of each peptide's contribution to the class differentiation.

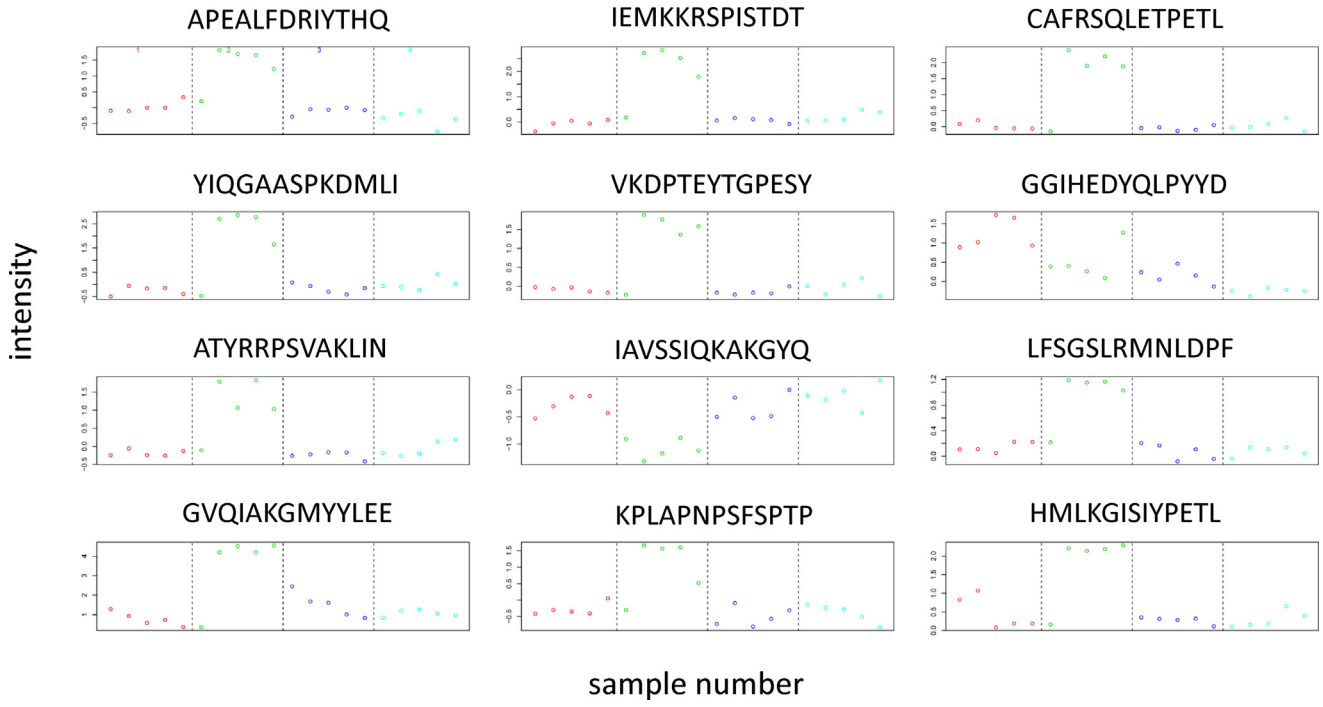


**Figure 3.** Intensity plot for the top peptides selected by PAM, grouped by time point. Red, green, blue, and cyan dots shown in the plots correspond to sample intensities at day 0, 56, 112, and 252, respectively.

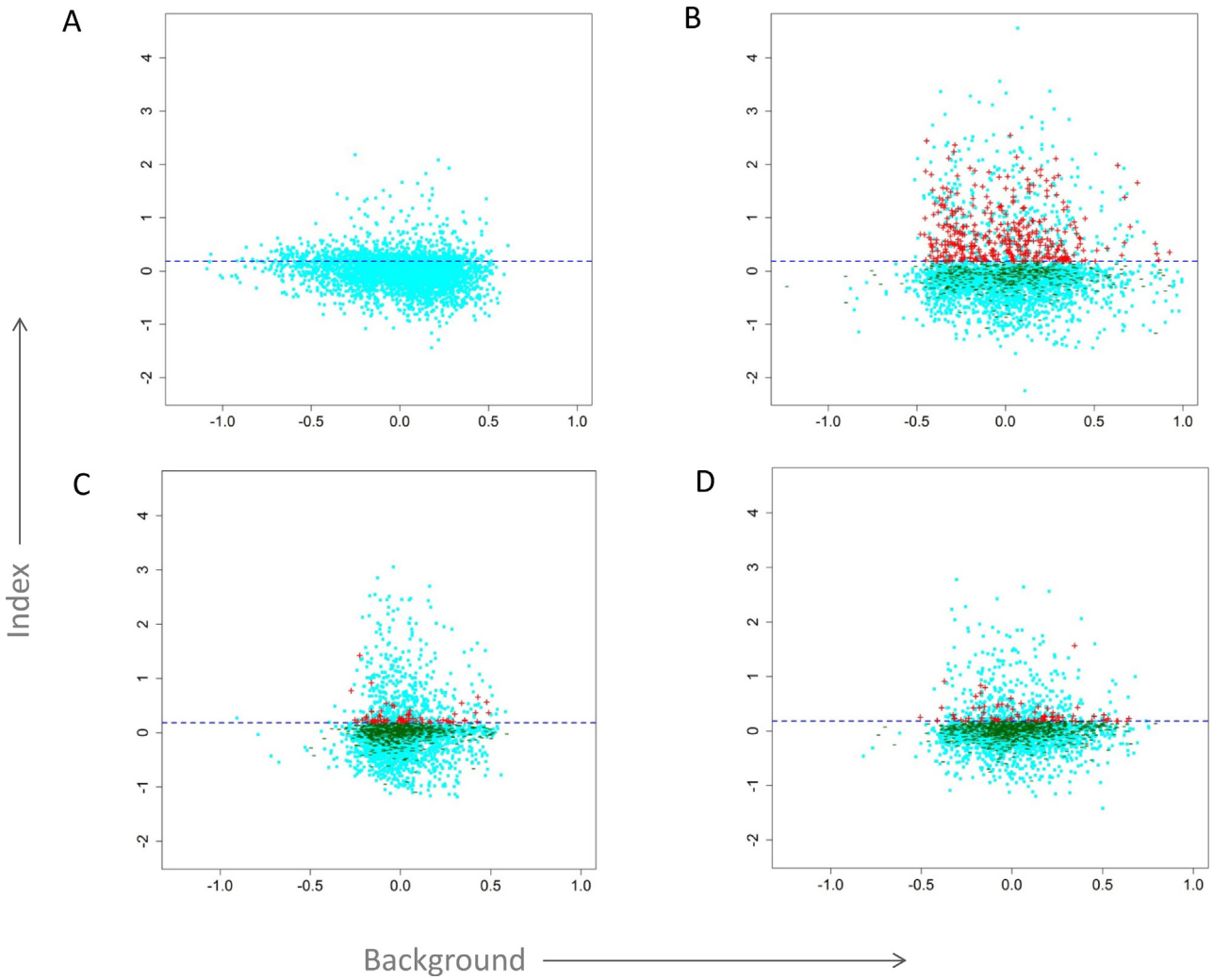


**Figure 4.** Scatter plots of intensities vs. log backgrounds for individual 1 at different time points. Shown are results for analyses at (A) time point 0; (B) time point day 56; (C) time point day 112; (D) time point day 252. New IgG-reactive peptides are marked in red, and peptides that are no longer recognized in green. The dashed line corresponds to the cut-off for recognition.

disease-specific immune responses previously reported in TB, autoimmune disease, and cancer.

'Non-specific' effects of BCG vaccination – contextually referring to immunological outcome other than mycobacteria-directed immune responses – have been described previously and attributed to the cross-reactivity observed in infants and neonates leading to protection against non-tuberculous pathogens.[30] Although the precise underlying mechanisms remain to be fully elucidated, the present study sheds some light on possible physiological processes that may be affected, and how these changes influence the immune system. The induction of measurable antibody, thus humoral immune responses to host proteins by the BCG vaccine, is a good indication of 'non-specific' immune-editing, as discussed in the preceding paragraphs. Nevertheless, vaccination of adults cannot be directly compared to very young children, and this hypothesis of course requires formal testing in healthy babies who receive the BCG vaccine for the first time. In addition, it is recognized that it would have been valuable for a control study to be performed alongside the present one – to gauge anti-BCG responses in the sera of the five vaccinated individuals described in this study; however, the availability of the serum samples that were provided was a limiting factor.

The results of the current study suggest that BCG vaccination modifies immunological and non-immunological host processes and may influence disease-specific immune responses. It would be interesting to investigate which of the physiological modifications in BCG-vaccinated adults may reveal opportunities in host-directed therapies (HDTs), and whether (host) antigen-specific humoral immune responses possibly enhance or decrease immune functions. Of note, although increased IgG reactivity occurred as a consequence of BCG vaccination, some antibody reactivity also disappeared. This was commonly seen at 56 days after vaccination. Although the 'absence' of immune reactivity to certain host targets is difficult to evaluate, it may have biologically and clinically relevant effects, e.g., suppression of certain B-cell clones that react to host proteins. This may be relevant in the case of autoimmune diseases, such as multiple sclerosis. In addition, the absence of certain host-directed IgG molecules has been associated with a high risk of developing neurological diseases, since naturally occurring antibodies aid in removing apoptotic cells – a mechanism that is crucial to maintaining neurological function.[53]

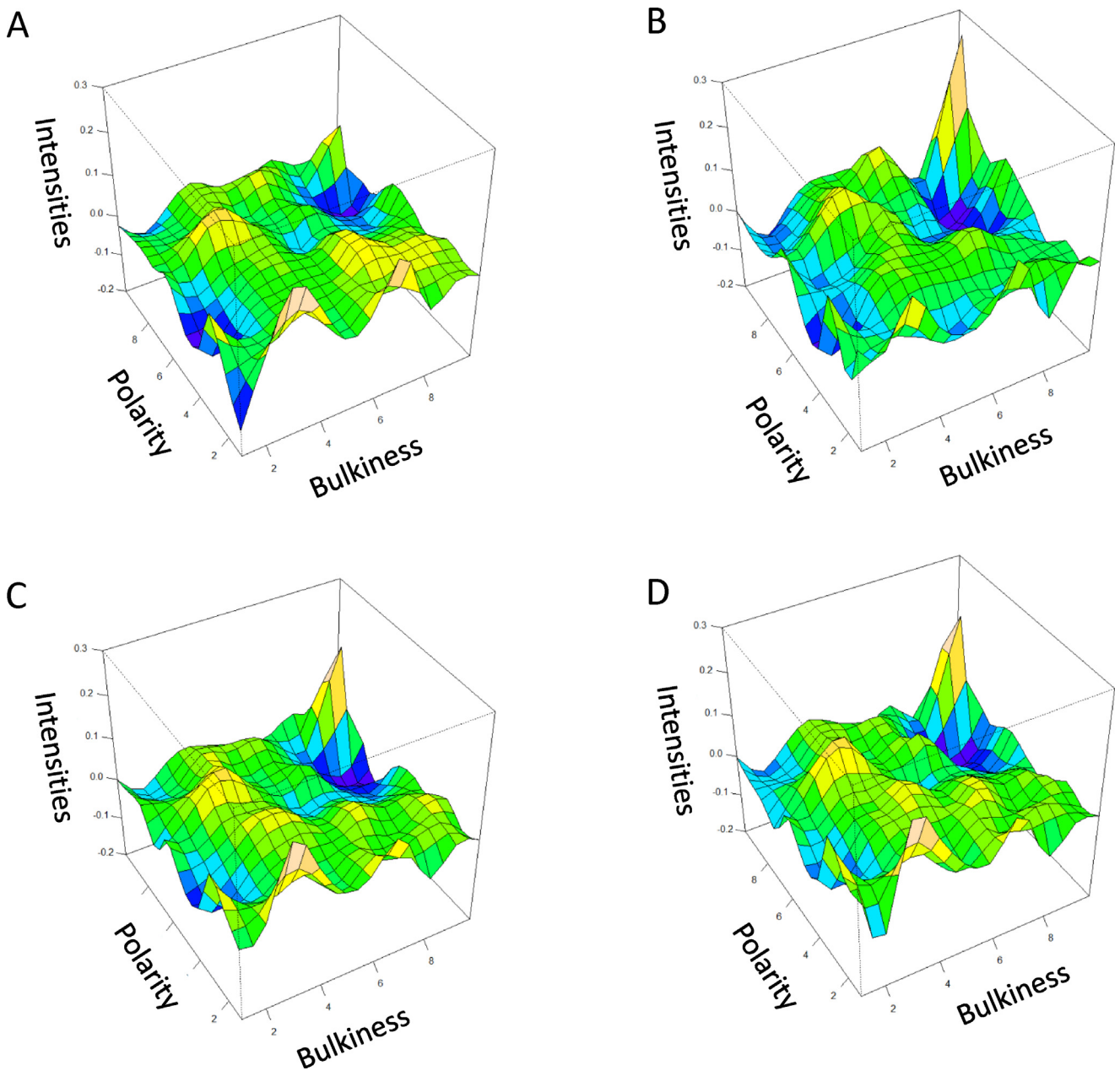


**Figure 5.** Bulkiness/polarity immune recognition surfaces.[27] Surfaces are computed at the four different time points post BCG vaccination: (a) day 0, (b) day 56, (c) day 112, (d) day 252.

BCG-induced immuno-editing can be harnessed to shape targeted immune responses in humans, taking into consideration the age of vaccine recipients, their general response to other vaccines, etc. It is also crucial to investigate which of the BCG-mediated modifications may reveal opportunities for HDTs.

In conclusion, using a human HCPM platform, changes in serum IgG reactivity to a panel of physiologically relevant host molecules following BCG vaccination of healthy adults were identified, which were most pronounced after 56 days of vaccination but waned after 112 and 252 days. BCG vaccination appears to induce immune-editing in the host by initially interrupting the proinflammatory response, followed by active suppression of anti-inflammatory factors. This pattern of BCG-induced responses may influence the modulation of targeted T-cell responses in health and disease, and provide opportunities for HDTs.

## Funding

This study was supported by grants from Vetenskapsrådet (Swedish Research Council), the Swedish International Cooperation Agency (SIDA), Söderberg Foundation, and Karolinska Institutet to MM.

## Conflict of interest

The authors declare no conflicts of interest.

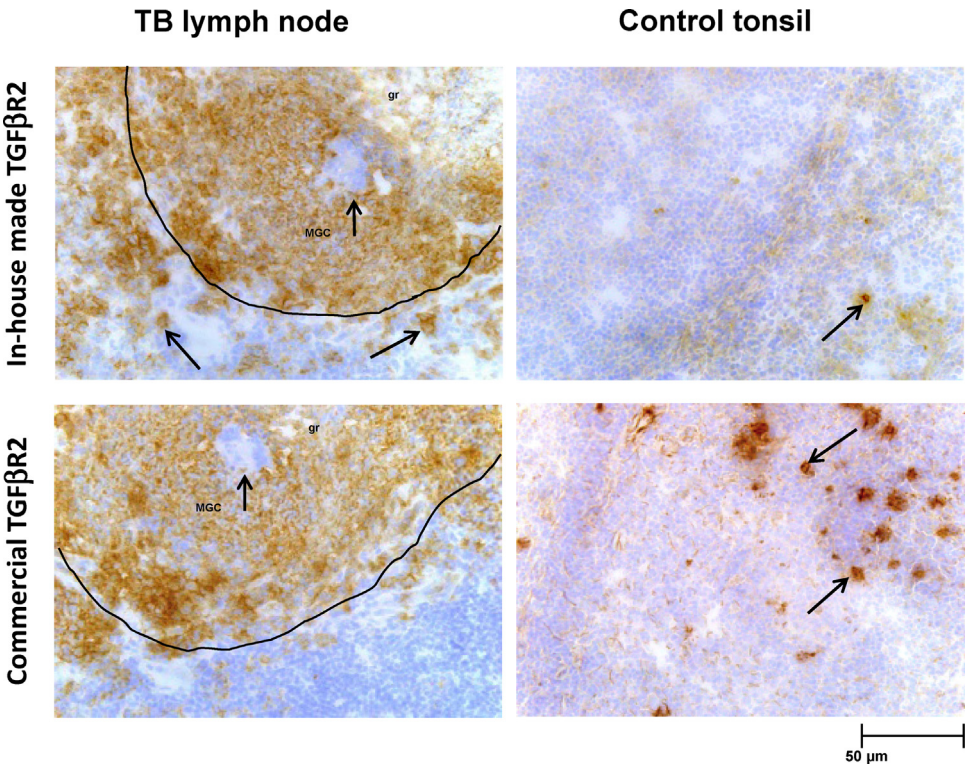


**Figure 6.** High expression of TGFβR2 in *Mycobacterium tuberculosis*-infected human lymph nodes. TGFβR2 protein immunostaining in human tissues with the monospecific antibody against GKQYWLITAFHAK (TGFβR2 epitope recognized in peptide microarray, custom-made), as well as a commercially available anti-human TGFβR2 antibody. The arrow heads indicate multinucleated giant cells (MGC), which are a characteristic trait of human TB granulomas (gr). Arrows indicate TGFβR-positive cells labelled in brown. Nuclear counterstaining with haematoxylin is shown in blue. Magnification is × 125. Representative images from five patients with TB lymphadenitis and five uninfected controls are shown.

## Appendix A. Supplementary data

Supplementary data associated with this article can be found, in the online version, at http://dx.doi.org/10.1016/j.ijid.2017.01.027.

## References


1. Luca S, Mihaescu T. History of BCG vaccine. *Maedica (Buchar)* 2013;**8**:6.
2. Roy A, Eisenhut M, Harris RJ, Rodrigues LC, Sridhar S, Habermann S, et al. Effect of BCG vaccination against *Mycobacterium tuberculosis* infection in children: systematic review and meta-analysis. *BMJ* 2014;**349**:g4643.
3. Favorov M, Ali M, Tursunbayeva A, Aitmagambetova I, Kilgore P, Ismailov S, Chorba T. Comparative tuberculosis (TB) prevention effectiveness in children of bacillus Calmette-Guerin (BCG) vaccines from different sources, Kazakhstan. *PLoS One* 2012;**7**:e32567.
4. Winters WD, Lamm DL. Antibody responses to bacillus Calmette–Guerin during immunotherapy in bladder cancer patients. *Cancer Res* 1981;**41**:2672–6.
5. Soares AP, Scriba TJ, Joseph S, Harbacheuski R, Murray RA, Gelderbloem SJ, et al. Bacillus Calmette–Guerin vaccination of human newborns induces T cells with complex cytokine and phenotypic profiles. *J Immunol* 2008;**180**:3569–77.
6. Achkar JM, Casadevall A. Antibody-mediated immunity against tuberculosis: implications for vaccine development. *Cell Host Microbe* 2013;**13**:250–62.
7. Behr MA, Wilson MA, Gill WP, Salamon H, Schoolnik GK, Rane S, Small PM. Comparative genomics of BCG vaccines by whole-genome DNA microarray. *Science* 1999;**284**:1520–3.
8. Vasekar M, Degraff D, Joshi M. Immunotherapy in bladder cancer. *Curr Mol Pharmacol* 2016;**9**(3):242–51.
9. Faustman DL, Wang L, Okubo Y, Burger D, Ban L, Man G, et al. Proof-of-concept, randomized, controlled clinical trial of bacillus Calmette–Guerin for treatment of long-term type 1 diabetes. *PLoS One* 2012;**7**:e41756.
10. Ristori G, Romano S, Cannoni S, Visconti A, Tinelli E, Mendozzi L, et al. Effects of bacille Calmette–Guerin after the first demyelinating event in the CNS. *Neurology* 2014;**82**:41–8.
11. Kaufmann SH, Cotton MF, Eisele B, Gengenbacher M, Grode L, Hesseling AC, Walzl G. The BCG replacement vaccine VPM1002: from drawing board to clinical trial. *Expert Rev Vaccines* 2014;**13**:619–30.
12. World Health Organization. *Global tuberculosis report 2015*. Geneva: WHO; 2015 p. 204.
13. Aguas A, Esaguy N, Sunkel CE, Silva MT. Cross-reactivity and sequence homology between the 65-kilodalton mycobacterial heat shock protein and human lactoferrin, transferrin, and DR beta subsets of major histocompatibility complex class II molecules. *Infect Immun* 1990;**58**:1461–70.
14. Shapira Y, Agmon-Levin N, Shoenfeld Y. *Mycobacterium tuberculosis*, autoimmunity, and vitamin D. *Clin Rev Allergy Immunol* 2010;**38**:169–77.
15. Lawrence DA. Transforming growth factor-beta: a general review. *Eur Cytokine Netw* 1996;**7**:363–74.
16. English K, Ryan JM, Tobin L, Murphy MJ, Barry FP, Mahon BP. Cell contact, prostaglandin E(2) and transforming growth factor beta 1 play non-redundant roles in human mesenchymal stem cell induction of CD4+CD25(High) forkhead box P3+ regulatory T cells. *Clin Exp Immunol* 2009;**156**:149–60.
17. Elias D, Britton S, Aseffa A, Engers H, Akuffo H. Poor immunogenicity of BCG in helminth infected population is associated with increased in vitro TGF-beta production. *Vaccine* 2008;**26**:3897–902.
18. Valentini D, Gaseitsiwe S, Maeurer M. Humoral 'reactome' profiles using peptide microarray chips. *Trends Immunol* 2010;**31**:399–400.
19. Gaseitsiwe S, Valentini D, Mahdavifar S, Magalhaes I, Hoft DF, Zerweck J, et al. Pattern recognition in pulmonary tuberculosis defined by high content peptide microarray chip analysis representing 61 proteins from *M. tuberculosis*. *PLoS One* 2008;**3**:e3840.
20. Reilly M, Valentini D. Visualisation and pre-processing of peptide microarray data. *Methods Mol Biol* 2009;**570**:373–89.
21. Valentini D, Ferrara G, Advani R, Hallander HO, Maeurer MJ. Serum reactome induced by *Bordetella pertussis* infection and pertussis vaccines: qualitative differences in serum antibody recognition patterns revealed by peptide microarray analysis. *BMC Immunol* 2015;**16**:40.
22. Ambati A, Valentini D, Montomoli E, Lapini G, Biuso F, Wenschuh H, et al. H1N1 viral proteome peptide microarray predicts individuals at risk for H1N1 infection and segregates infection versus Pandemrix((R)) vaccination. *Immunology* 2015;**145**:357–66.
23. Nahtman T, Jernberg A, Mahdavifar S, Zerweck J, Schutkowski M, Maeurer M, Reilly M. Validation of peptide epitope microarray experiments and extraction of quality data. *J Immunol Methods* 2007;**328**:1–13.
24. Tusher VG, Tibshirani R, Chu G. Significance analysis of microarrays applied to the ionizing radiation response. *Proc Natl Acad Sci U S A* 2001;**98**:5116–21.

25. Phipson B, Lee S, Majewski IJ, Alexander WS, Smyth GK. Robust hyperparameter estimation protects against hypervariable genes and improves power to detect differential expression. *Ann Appl Stat* 2016;**10**:946–63.
26. Tibshirani R, Hastie T, Narasimhan B, Chu G. Diagnosis of multiple cancer types by shrunken centroids of gene expression. *Proc Natl Acad Sci U S A* 2002;**99**:6567–72.
27. Valentini D, Rao M, Ferrara G, Perkins M, Dodoo E, Zumla A, Maeurer M. Immune recognition surface construction of Mycobacterium tuberculosis epitope-specific antibody responses in tuberculosis patients identified by peptide microarrays. *Int J Infect Dis* 2017 Feb 9. pii: S1201-9712(17)30018-8.
28. Brachtel EF, Washiyama M, Johnson GD, Tenner-Racz K, Racz P, MacLennan IC. Differences in the germinal centres of palatine tonsils and lymph nodes. *Scand J Immunol* 1996;**43**:239–47.
29. Rahman S, Gudetta B, Fink J, Granath A, Ashenafi S, Aseffa A, et al. Compartmentalization of immune responses in human tuberculosis: few CD8+ effector T cells but elevated levels of FoxP3+ regulatory t cells in the granulomatous lesions. *Am J Pathol* 2009;**174**:2211–24.
30. Aaby P, Kollmann TR, Benn CS. Nonspecific effects of neonatal and infant vaccination: public-health, immunological and conceptual challenges. *Nat Immunol* 2014;**15**:895–9.
31. Hanekom WA. The immune response to BCG vaccination of newborns. *Ann N Y Acad Sci* 2005;**1062**:69–78.
32. Askeland EJ, Newton MR, O'Donnell MA, Luo Y. Bladder cancer immunotherapy: BCG and beyond. *Adv Urol* 2012;**2012**:181987.
33. Ravn P, Boesen H, Pedersen BK, Andersen P. Human T cell responses induced by vaccination with *Mycobacterium bovis* bacillus Calmette–Guerin. *J Immunol* 1997;**158**:1949–55.
34. Elsasser J, Janssen MW, Becker F, Suttmann H, Schmitt K, Sester U, et al. Antigen-specific CD4T cells are induced after intravesical BCG-instillation therapy in patients with bladder cancer and show similar cytokine profiles as in active tuberculosis. *PLoS One* 2013;**8**:e69892.
35. Lo WL, Donermeyer DL, Allen PM. A voltage-gated sodium channel is essential for the positive selection of CD4(+) T cells. *Nat Immunol* 2012;**13**:880–7.
36. Russell SM, Johnston JA, Noguchi M, Kawamura M, Bacon CM, Friedmann M, et al. Interaction of IL-2R beta and gamma c chains with Jak1 and Jak3: implications for XSCID and XCID. *Science* 1994;**266**:1042–5.
37. Zhu X, Marcus WD, Xu W, Lee HI, Han K, Egan JO, et al. Novel human interleukin-15 agonists. *J Immunol* 2009;**183**:3598–607.
38. Byrd VM, Kilkenny DM, Dikov MM, Reich MB, Rocheleau JV, Armistead WJ, et al. Fibroblast growth factor receptor-1 interacts with the T-cell receptor signalling pathway. *Immunol Cell Biol* 2003;**81**:440–50.
39. Edling CE, Hallberg B. c-Kit—a hematopoietic cell essential receptor tyrosine kinase. *Int J Biochem Cell Biol* 2007;**39**:1995–8.
40. Langley AR, Chambers H, Christov CP, Krude T. Ribonucleoprotein particles containing non-coding Y RNAs, Ro60, La and nucleolin are not required for Y RNA function in DNA replication. *PLoS One* 2010;**5**:e13673.
41. Franceschini F, Cavazzana I. Anti-Ro/SSA and La/SSB antibodies. *Autoimmunity* 2005;**38**:55–63.
42. Goeb V, Salle V, Duhaut P, Jouen F, Smail A, Ducroix JP, et al. Clinical significance of autoantibodies recognizing Sjögren's syndrome A (SSA), SSB, calpastatin and alpha-fodrin in primary Sjögren's syndrome. *Clin Exp Immunol* 2007;**148**:281–7.
43. Allen SS, Cassone L, Lasco TM, McMurray DN. Effect of neutralizing transforming growth factor beta1 on the immune response against *Mycobacterium tuberculosis* in guinea pigs. *Infect Immun* 2004;**72**:1358–63.
44. Roberts T, Beyers N, Aguirre A, Walzl G. Immunosuppression during active tuberculosis is characterized by decreased interferon-gamma production and CD25 expression with elevated forkhead box P3, transforming growth factor-beta, and interleukin-4 mRNA levels. *J Infect Dis* 2007;**195**:870–8.
45. Eiden LE, Schafer MK, Weihe E, Schutz B. The vesicular amine transporter family (SLC18): amine/proton antiporters required for vesicular accumulation and regulated exocytotic secretion of monoamines and acetylcholine. *Pflugers Arch* 2004;**447**:636–40.
46. Tritsch NX, Ding JB, Sabatini BL. Dopaminergic neurons inhibit striatal output through non-canonical release of GABA. *Nature* 2012;**490**:262–6.
47. Lin L, Yee SW, Kim RB, Giacomini KM. SLC transporters as therapeutic targets: emerging opportunities. *Nat Rev Drug Discov* 2015;**14**:543–60.
48. Zhu Q, Zhang M, Shi M, Liu Y, Zhao Q, Wang W, et al. Human B cells have an active phagocytic capability and undergo immune activation upon phagocytosis of *Mycobacterium tuberculosis*. *Immunobiology* 2016;**221**:558–67.
49. Rao M, Valentini D, Poiret T, Dodoo E, Parida S, Zumla A, et al. B in TB: B cells as mediators of clinically relevant immune responses in tuberculosis. *Clin Infect Dis* 2015;**61**(Suppl 3):S225–34.
50. Achkar JM, Chan J, Casadevall A. B cells and antibodies in the defense against *Mycobacterium tuberculosis* infection. *Immunol Rev* 2015;**264**:167–81.
51. Axelsson-Robertson R, Ju JH, Kim HY, Zumla A, Maeurer M. *Mycobacterium tuberculosis*-specific and MHC class I-restricted CD8+ T-cells exhibit a stem cell precursor-like phenotype in patients with active pulmonary tuberculosis. *Int J Infect Dis* 2015;**32**:13–22.
52. Zumla A, Rao M, Parida SK, Keshavjee S, Cassell G, Wallis R, Axelsson-Robertsson R, Doherty M, Andersson J, Maeurer M. Inflammation and tuberculosis: host-directed therapies. *J Intern Med.* 2014;**277**(April (4)):373–87.
53. Britschgi M, Olin CE, Johns HT, Takeda-Uchimura Y, LeMieux MC, Rufibach K, et al. Neuroprotective natural antibodies to assemblies of amyloidogenic peptides decrease with normal aging and advancing Alzheimer's disease. *Proc Natl Acad Sci U S A* 2009;**106**:12145–50.